

Citation: Ngun Za Iang, S. Kita (2019), Completeness Magnitude of Earthquakes and b-Value in Myanmar, Synopsis of IISEE-GRIPS master report.

# COMPLETENESS MAGNITUDE OF EARTHQUAKES AND b-VALUE IN MYANMAR

Ngun Za Iang<sup>1,2</sup>

Supervisor: Saeko KITA<sup>3</sup>

## ABSTRACT

In order to estimate completeness magnitude of earthquakes and b-values, the NEDC local dataset was used during 2014-2018. This study aims to estimate the completeness magnitude of earthquakes in Myanmar and to examine the b-value with its relations: depth, faulting style, and stress accumulating in a sophisticated tectonic setting of Myanmar. The completeness magnitude  $M_c$  was estimated as ML 2.8 with a b-value  $0.68 \pm 0.02$  in the whole study region. Regionally, the b-values vary from 0.52 to 1.0. The tendency relation between b-value and faulting styles was found along the Sagaing Fault. The southern part with a smaller b-value indicates a thrust mechanism, whereas the northern part with a larger b-value shows a strike-slip mechanism. The b-value generally increases with the increase of depth in the whole study region. In the active fault region, the b-value decreases with depth within the upper crust at depths of  $\sim 15$  km, which might be related to high-stress accumulation. Below at a depth of 15 km, the b-value then increases with a function of depth. In contrast, a significant decrease of b-value with depth was observed at depths of 75-85 km in the subduction zone of the study region, which might be discussed with the process of dehydration in the ocean crust. The methodology of this study might be fruitful to understand the seismically complex tectonic system beneath Myanmar.

**Keywords:** b-value, completeness magnitude, maximum likelihood method, stress, Myanmar.

## 1. INTRODUCTION

b-value is one of the most functional seismic parameters to study the seismicity within a specified region and time window. The b-value is calculated from Gutenberg and Richter (1944) frequency-magnitude distribution as  $\log_{10} N = a - bM^{min}$ , where  $N$  is the cumulative number of earthquakes with the magnitude  $M$  ( $\geq M^{min}$ ), ' $a$ ' and ' $b$ ' are constants. The parameter ' $a$ ' is related to seismic activities, depending on many parameters; the size of the region, time intervals, a total number of earthquakes and its magnitude and the value of ' $b$ '. ' $b$ ' is the b-value, indicating the slope of the cumulative number against magnitude. To understand seismic characteristics, previous studies have revealed b-value and its correlations: heterogeneous materials (Mori and Abercrombie, 1997), focal mechanism dependence (Schorlemmer et al., 2005), dependence of depths and strength profile of the crust (Spada et al., 2013), the age of a subducting plate (Nishikawa and Ide, 2014) and differential stress (Scholz, 2015). Nanjo et al. (2019) and Nanjo et al. (2012) indicated that the b-values of earthquakes in the Kumamoto and Tohoku-Oki decrease just before the mainshocks, respectively. Therefore, the examination of b-values of events can offer valuable information about the future activity of earthquakes in the specific region.

---

<sup>1</sup> Department of Meteorology and Hydrology (DMH), Myanmar.

<sup>2</sup> IISEE-GRIPS master course student

<sup>3</sup> International Institute of Seismology and Earthquake Engineering, Building Research Institute.

Myanmar is one of the most earthquake-prone regions, located in the Alpidic Himalayan Seismic Belt. Mainly, four tectonic plates exist in and around Myanmar: The Eurasian, the Indian, the Sunda, and the Burma Plates (Hurukawa et al., 2012) as shown in Figure 1. Also, the Indian Plate subducts beneath the Burma Plate. Moreover, the Sagaing Fault is a major active fault, located as a boundary between the Burma and Sunda Plates, and runs over 1000 km from north to south. It is a right-lateral strike-slip fault with a displacement rate of 18 mm/yr (Socquet et al., 2006). Due to the seismically complex tectonic system, the shallow to intermediate-focus earthquakes occurred in the subduction zone (the western part), whereas most of the shallow earthquakes occurred in the active fault region (the eastern part) as shown in Figure 1. In order to comprehend characteristic of seismic activities beneath in Myanmar, the main goal is to estimate the magnitude of completeness of earthquakes in Myanmar using the dataset of National Earthquake Data Center (NEDC) and to evaluate b-value with its correlations: depth, focal mechanisms and stress accumulation in the study region.

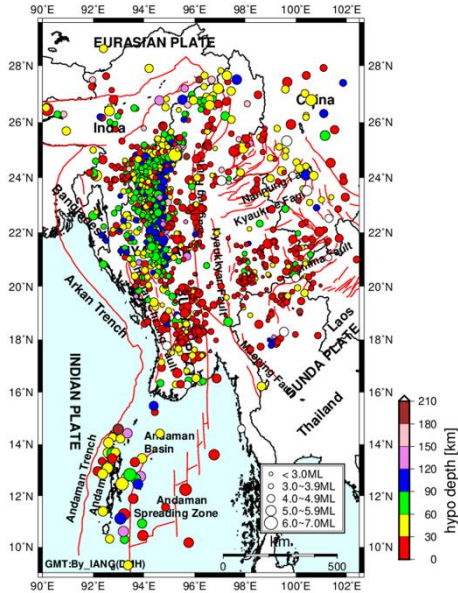


Figure 1. The tectonic setting of Myanmar and neighbor regions (Hurukawa et al. (2012) and Wang et al. (2014)) and epicenters of events during 201-2018 (NEDC).

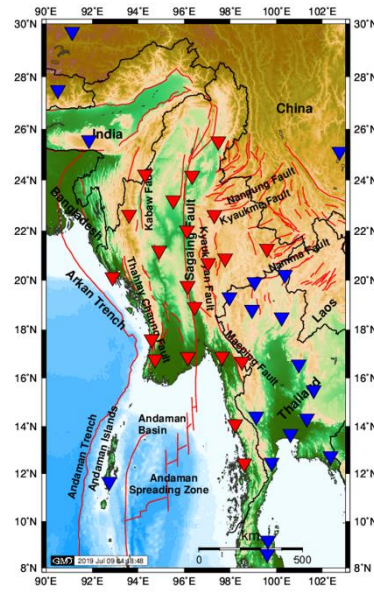


Figure 2. Locations of broadband seismic stations (inverted-red triangles) in Myanmar and neighbor countries' stations (inverted-blue triangles). Red lines: Active faults.

## 2. METHODOLOGY

To evaluate the b-value, the maximum likelihood method (Utsu, 1965) was adopted as follows;

$$b = \frac{\log_{10} e}{\overline{M} - M_c}, \quad (1)$$

where  $\overline{M}$  is the average magnitude of cumulative earthquakes with  $M > M_c$ .  $M_c$  is the magnitude of completeness or the smallest earthquake magnitude and  $\log_{10} e = 0.4343$ . A larger b-value corresponds to smaller events while a smaller b-value is related to larger events.

Moreover, to calculate the error  $\delta b$  of b-value, the method developed by Aki (1995) was used as follows;

$$\delta b = b / \sqrt{N}, \quad (2)$$

where  $N$  is the total number of earthquakes of the given sample.

The goodness-of-fit method (Wiermer and Wyss, 2000) was also used to estimate  $M_c$  by computing the absolute difference  $R$  of the number of events in each magnitude bin as follows;

$$R(a, b, M_i) = 100 - \left( \frac{\sum_i^{M_i} |B_i - S_i|}{\sum_i B_i} 100 \right), \quad (3)$$

where  $B_i$  and  $S_i$  are the observed and predicted cumulative number of events in each magnitude bin.

### 3. DATA

A total of 21 broadband seismic stations has been installed throughout Myanmar between 2008 and 2018 (Figure 2), which provide a valid dataset with local magnitude (ML) within a distance of 1,000 km (Shiddiqi et al., 2019). Since 2014, the Department of Meteorology and Hydrology (DMH) has been using SEISAN program developed by Havskov and Ottemoller (2010) from the University of Bergen to determine hypocenter locations and magnitude of events. The study area was selected between the latitudes of 16-28° N and the longitudes of 92-102° E depending on including the number of events within the study period (2014-2018). This study could not cover the Andaman Islands region due to the limitation of event number during this study. A total of 1350 events was collected from the NEDC local dataset with local magnitude listed from 1.0-6.3 (ML) to estimate  $M_c$  and  $b$ -values. Moreover, 197 events were also collected from the Global Centroid Moment Tensor Catalog between 2009 and 2018 to investigate focal mechanism solutions which show faulting styles.

### 4. RESULTS AND DISCUSSIONS

#### 4.1. Completeness Magnitude and $b$ -Value Estimation in the Whole Study Region

By using the NEDC local data (2014-2018), including 1350 events of homogeneous magnitude (ML), the magnitude of completeness was estimated as ML 2.8 with 690 events and a  $b$ -value  $0.68 \pm 0.02$  in the whole study region (Figure 3). When the change of  $M_c$  with time was calculated by using a three-year window, the  $M_c$  decreases with time during this study period (Figure 4). The decrease of  $M_c$  with time might be related to the improvement of local seismic networks in Myanmar during this study period. A total of 690 events satisfied  $M_c$  2.8 was taken as a final database to estimate the  $b$ -values in this study (Figure 5).

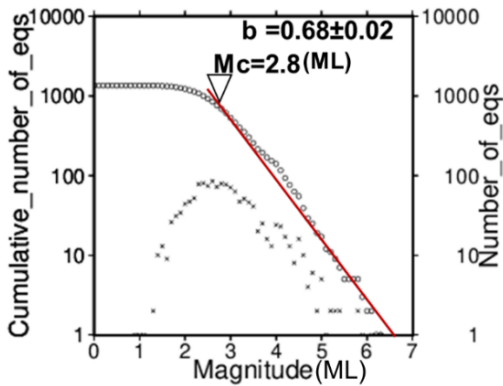


Figure 3. Estimation of  $b$ -value and  $M_c$  in the whole study region. Solid red line: the line of the best fit. Circles: the cumulative number of events. Crosses: the number of events of each magnitude.

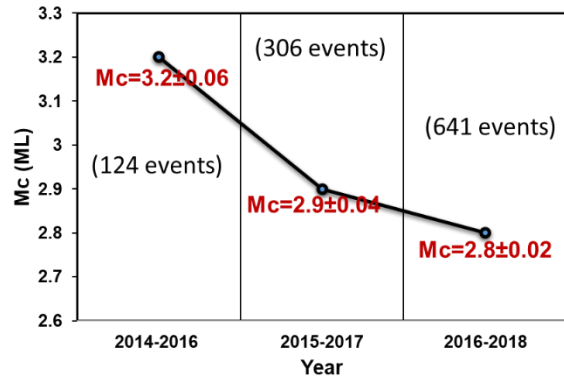


Figure 4. The change of  $M_c$  with time during this study period (2014-2018). ML: Local Magnitude.

## 4.2. Regional Variations of b-values in the Study Region

To examine differences of b-values between the subduction and active fault regions, the study region (Figure 5) was divided into three sub-regions: the western part (the subduction region) between the latitudes of 16-28° N and the longitudes of 92-95.4° E, the region along the Sagaing Fault between the latitudes of 16-28° N and the longitudes of 95.4-97.5° E and the eastern part (active fault region), the latitudes of 16-28° N and the longitudes of 97.5-102° E. Then the b-values were obtained as  $0.74\pm 0.03$  in the subduction region,  $0.62\pm 0.05$  in the region along the Sagaing Fault and  $0.65\pm 0.06$  in the eastern part respectively. The b-value of the subduction region is higher than that of other active fault regions. Oncel et al. (2001) also showed that lower b-values are associated with the increase of possible occurrence of more significant future earthquakes because of the concentration of stress in the extremely faulted area.

Moreover, when dividing the study region (Figure 5) into four, the b-values were obtained as:  $0.74\pm 0.03$  in the northwestern part between 22-28° N and 92-97° E,  $0.66\pm 0.05$  in the southwestern part between 16-22° N and 92-97° E,  $0.52\pm 0.06$  in the northeastern part between 22-28° N and 97-102° E and  $1.0\pm 0.13$  in the southeastern part between 16-22° N and 92-97° E, respectively. The variations of b-values from 0.52 to 1.0 in this study might be related to regional stress variations resulting from the characteristics of the tectonic plate and active fault.

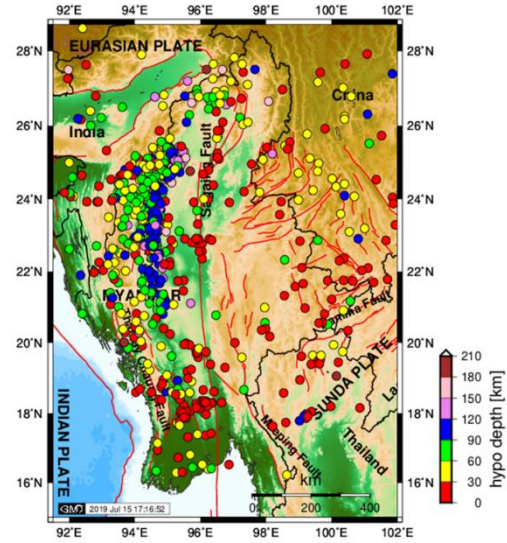


Figure 5. The epicenter locations of selected 690 events ( $ML \geq 2.8$ ) within the study region, from the NEDC dataset (2014-2018). Red lines: Active faults.

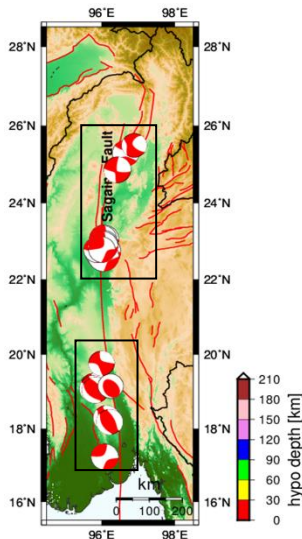


Figure 6. Focal mechanism solutions (global CMT catalog) of events along the Sagaing Fault.

depth. The depth histogram (Figure 8) showing the decrease of event number with depth might affect the increase of b-values with depths as well. The b-value slightly decreases within the depths of ~15 km, and below at 15 km depth, the b-value increases with depth. The lower b-value within the upper crust may be associated with the higher accumulation of stress because the b-value is negatively correlated to stress. Spada et al. (2013) also indicated that the b-value decrease within the brittle upper crust before

Moreover, the tendency correlation of b-values and faulting styles was also found along the Sagaing Fault (Figure 6). The b-value in the southern part containing thrust mechanisms is  $0.61\pm 0.07$ , whereas the b-value in the northern part showing strike-slip mechanism is  $0.67\pm 0.07$  (Table 1). Schorlemmer et al. (2005) also indicated that the b-values of thrust mechanisms are lower than those of strike-slip mechanisms.

Table 1. Difference of b-values along the Sagaing Fault.

Region	b-value	Error
Northern part	0.67	0.07
Southern part	0.61	0.07

## 4.3. Regionally Variations of b-Values with depths

In the whole study region, the variation of b-values with depths was calculated by using moving 5 km depth with 150 events in each bin starting from the surface to the depth of 150 km (Figure 7). Generally, the trend of b-values increases with the increase of

stopping the decrease in depth near the brittle-ductile transition zone, and increases in the deeper depths again.

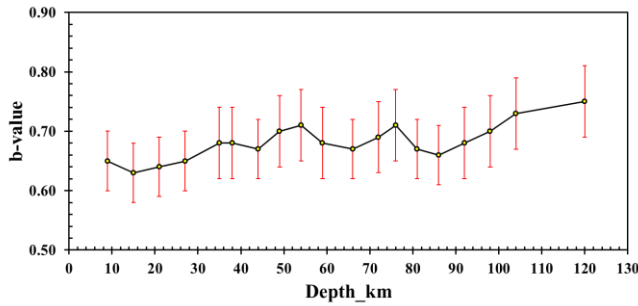


Figure 7. Variation of b-values (yellow circles) with depth and its error (red vertical bar) in the whole study region.

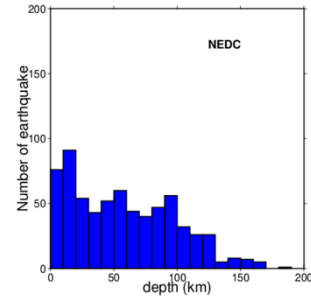


Figure 8. Depth histogram of the selected 690 events ( $ML \geq 2.8$ ).

Moreover, the variation of b-values with depths was examined depending on the difference of tectonic features. In the active fault regions, the variation of b-values with depths was examined by using moving 5 km depth with a 50-event bin due to the limitation of event number during this study. As a result, the b-value decreases within depths of  $\sim 15$  km, and below at a depth of 15 km, the b-value increases with the increase of depth (Figure 9). Moreover, the depth histogram of events (Figure 10) of the active fault regions shows the decrease of event number with depth below at a depth of 20 km.

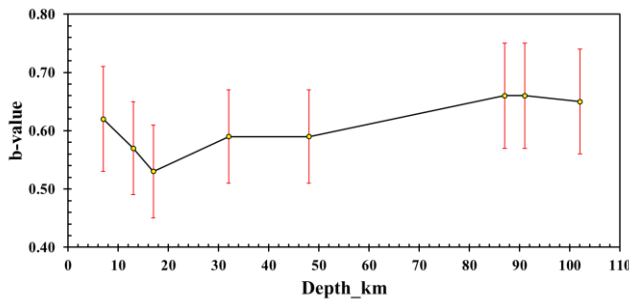


Figure 9. Variation of b-values (yellow circles) with depth and its error (red vertical bar) in the Sagaing Fault region.

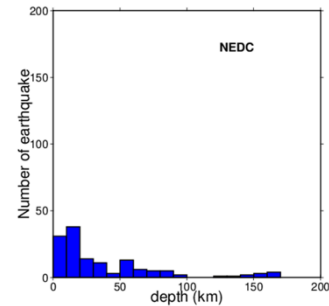


Figure 10. Depth histogram of events ( $ML \geq 2.8$ ) in the Sagaing Fault region.

When the variation of b-values was examined in the subduction region, the computation was performed by using moving 5 km depth with a 100-event bin. In contrast, a significant decrease of b-value was observed at depths of 75-85 km, which is similar with the result of the whole study region showing the decrease at depths of 80-85 km (Figure 6). Shiddiqi et al. (2018) reported that the source process of the Chauk earthquake ( $M_w$  6.8) with an intraslab intermediate-depth of 84.1 km, which shows sub horizontal mechanism faulting, corresponds to the dehydration fragility. The significant lower b-value at depths of 75-85 km might be associated with the hypocenter depth of the Chauk earthquake (at a depth of 84.1 km) as well as the process of dehydration fragility at intraslab intermediate-depths.

## 5. CONCLUSIONS

In this study, the b-value and the completeness magnitude  $M_c$  of earthquakes in Myanmar were estimated by analyzing the NEDC local dataset (2014-2018) and obtained  $M_c$  2.8 (ML) and  $b=0.68 \pm 0.02$  in the whole study region. The  $M_c$  also decreases with time. Moreover, by investigating the regional variation of b-values, the b-values vary from 0.52 to 1.0. The b-value of the active fault region is lower

than that of the subduction region, which could show higher stress accumulation in the active fault region than the subduction region. Besides, the tendency correlation of b-values and different faulting styles was investigated along the Sagaing Fault. The southern part of the Sagaing Fault related a smaller b-value shows thrust mechanisms, whereas the northern part of the Sagaing Fault correspondent to a larger b-value indicates strike-slip mechanisms.

Furthermore, when the temporal variation of b-values as a function of depths in the study region was explored, generally, the b-value trend increases with respect to depth in the whole region. In the active fault region, the b-value decreases with depth within the brittle upper crust at depths of ~15 km, and the decrease of b-value stops near the brittle-ductile transition, which shows the higher stress accumulation in the upper crustal rock. Then below 15 km, the b-value increases with the increase of depth. In contrast, a significant decrease of b-value was found at intraslab intermediate- depths of 75-85 km in the subduction zone.

This study shows that the examination of b-values and following procedure are useful for evaluating seismic observation network and understanding seismic activities in Myanmar. The installation of the local seismic observation networks might play an essential role in the study of seismic hazard assessment and the mitigation of devastating natural disasters caused by earthquakes in earthquake-prone regions.

### ACKNOWLEDGEMENTS

This research was conducted during the individual study period of the training course “Seismology, Earthquake Engineering and Tsunami Disaster Mitigation” by the Building Research Institute, JICA, and GRIPS. I am deeply thankful to my advisor and supervisor, Dr. Saeko KITA, for always giving valuable advice and guiding me to complete my individual study successfully. I would like to express my gratitude to Dr. Tatsuhiko HARA and Dr. Bunichino SHIBAZAKI for their invaluable suggestion throughout my research work. I would like to express thanks to all JICA and IISEE/ BRI staff members for their support and encouragement through this training course. I am grateful to GRIPS for giving me a chance to attend this master course.

### REFERENCES

- Aki, K., 1995, *Bull. Earthquake Res. Inst. Tokyo Univ.*, 43, 237-239.
- Gutenberg, B., and Richter, C.F., 1944, *Bull. Seism. Soc. Am.*, 34, 185-188.
- Havskov, J. and Ottemoller, L., 2010, *Spring*, doi: 10.1007/978-90-481-8697-6.
- Hurukawa, N., Tun, P.P and Shibazaki, B., 2012, *Earth Planets Space*, 56, 333-343.
- Mori, J. and Abercrombei, R.E., 1997, *Jour. Geo. Res.*, Vol. 102, No. B7, pages 15,081-15,090.
- Nanjo, K.Z., Hirata, N., Obara, K. and Kasahara, K., 2012, *Geophys. Res. Lett.* 39, L20304.
- Nanjo, K.Z., Izutsu, J., Orihara, Y., Kamogawa, M. and Nagao, T., 2019, *Am. Geo. Union.*, doi: 10.1029/2019GL083463.
- Nishikawa, T and Ide, S., 2014, *Nature*, doi: 10.1038/NGEO2279.
- Siddiqi, H.A., Tun, P.P., Kyaw, T.L. and Ottemoller, L., 2018, *Seism. Res. Lett.*, Vol. 89, No. 5.
- Siddiqi, H.A., Tun, P.P. and Ottemoller, L., 2019, *Seism. Res. Lett.*, doi: 10.1785/0220190065.
- Socquet, A., Vigny, C., Chamot-Rooke, N., Simons, W., Rangin, C. and Ambrosius, B., 2006, *Jour. Geo. Res.* Vol. 111, B05406.
- Scholz, C.H., 2015, *Geophys. Res. Lett.*, 42, 1399-1402.
- Schorlemmer, D., Wiermer, S. and Wyss, M., 2015, *nature*, doi:10.1038/nature04094.
- Spada, M., Tormann, T., Wiermer, S. and Enescu, B., 2013, *Geophys. Res. Lett.*, Vol. 40, 709-714.
- Utsu, T., 1965, *Geophys. Bull. Hok-kaido Univ.*, Hokkaido, Japan, 13, 99-103.
- Wang, Y., Seih, K., Tun, S.T., Lai, K.Y. and Myint, T., 2014, *Jour. Res.*, 199(4), 3767-3822.
- Wiermer, S. and Wyss, M., 2000, *Bull. Seism. Am.*, 90, 4, p. 859-869.
- Web site: CMT Catalog, <https://www.globalcmt.org/CMTsearch>.